

# *Anopheles gambiae* (Ag55) cells are phagocytic and have hemocyte-like gene expression

Michael J. Adang (✉ [adang@uga.edu](mailto:adang@uga.edu))

University of Georgia

Ruchir Mishra

University of Florida

Gang Hua

University of Georgia

Urjwal R. Bagal

University of Georgia

Don Champagne

University of Georgia

---

## Research article

**Keywords:** *Anopheles gambiae*, next generation sequencing, flow-cytometry, phagocytosis, hemocyte-like, confocal microscopy, FPKM

**Posted Date:** February 27th, 2020

**DOI:** <https://doi.org/10.21203/rs.2.24674/v1>

**License:**  This work is licensed under a Creative Commons Attribution 4.0 International License.

[Read Full License](#)

---

## Abstract

Background *Anopheles gambiae* is the predominant vector of malaria, the fourth largest cause of infant mortality, in sub-Saharan Africa. Furthermore, *A. gambiae* is also the primary vector of O'nyong-nyong virus. The complexity of handling *A. gambiae* and infectious pathogens has led to the use of *A. gambiae* cell lines, including Ag55 cells, as a potential model to study vector-pathogen interactions and immune responses. The utility of cell lines can be maximized if their detailed gene expression profile and properties are available.

Results We provide detailed gene expression profiles, proteome and information about the properties of Ag55 cells. KEGG pathway analysis on genes with transcript levels of  $\geq 200$  FPKM revealed phagosome term enriched. Further, transcriptomic data backed by confocal microscopy and flow cytometry suggest that Ag55 cells have are hemocyte-like with phagocytic properties and immune competence.

Conclusion As Ag55 cells are immune competent and express hemocyte like properties they can be used as a model to study vector-pathogen immune response. Furthermore, the availability of transcriptomic data of Ag55 cells will help researchers use and engineer the Ag55 cell line in an efficient way, for example by developing strategies to make it more suitable for studies of interactions with *Plasmodium* and other microbes.

## Background

*Anopheles gambiae* is the predominant vector of malaria in Africa, which is caused by an apicomplexan belonging to the genus *Plasmodium*. In 2018, 214 million cases of malaria were reported world-wide, of which 88% of those cases were in Africa, predominately sub-Saharan Africa where malaria was the fourth largest cause of infant mortality [1]. *Anopheles gambiae* also vectors O'nyong-nyong arbovirus and other viruses that pose emerging threats to human health.

The vectorial capacity of mosquitoes to transmit infectious pathogens depends on many pathogen-host interactions such as pathogen entry and development in the host, each of which is countered by the innate immune response of the host [2-5]. Environmental factors provide challenges for studying mosquito-infectious microbe interactions at the whole animal level. The handling of mosquitoes and infectious pathogens requires a range of skills and facilities including the ability to raise large numbers of mosquitoes, facilities for handling both the insect vector and the pathogen and expertise in vector and pathogen biology. Mosquito cell lines have been used as models to investigate mosquito pathogen interactions [6-8].

Mosquito cell lines have been used to investigate mosquito-virus interactions [6, 7, 9], as models for deducing the host range of arboviruses [10, 11], for isolating and characterizing mosquito-specific flaviviruses [12, 13], for the potential *in vitro* development of *Plasmodium* ookinetes [14, 15], and for screening of insecticides [16]. High throughput RNAi screens have made cell lines useful models for

been shown to correlate well with experiments using whole flies for genetic and developmental studies [20-23]. *A. gambiae* cell lines have been used as models to study mosquito immune responses [24-27]. Further, these cells have been shown to express immune factors upon microbial challenge and perform complex immune tasks such as phagocytosis of beads and bacteria [24, 28]. The discovery of *A. gambiae* densonucleovirus (AgDNV) is important as this virus replicates in adult mosquitoes and in cultured *An. gambiae* MOS55 cells with minimal physiological effects on the host. It is likely that AgDNV can be engineered as a transducing virus.

Cell lines have been derived from *A. gambiae* as it is the primary vector of malaria in sub-Saharan Africa. The Ag55 [29], Sua1B and Sua4a-3B [25] cell lines are derived from neonate first instar larvae. Further, a Sua5B cell line was derived by splitting Sua1 cell line [30]. The Sua1B, Sua4a-3B, and Sua5B cell lines are considered to have hemocyte-like properties [25, 30].

*Anopheles* Ag55 cells were tested as a model to study *Plasmodium* ookinete interaction [8], and *Lysinibacillus sphaericus* Bin toxin mode of action [31]. Ag55 cells are amenable to RNA inhibition-based knock-down of targeted mosquito genes [32, 33]. We used transcriptomic analyses, confocal microscopy and flow cytometry towards the goal of enhancing the utility of Ag55 cells for pathogen interaction, genetic and immune response studies. KEGG analysis of genes with transcripts level  $\geq 200$  FPKM identified phagosome term enriched. Confocal microscopy images and flow cytometry data showed internalization of FITC-*E.coli* bioparticles. The presence of phagocytic receptors, hemocyte markers and anti-microbial peptide transcripts suggest Ag55 cells have hemocyte like properties.

## Results And Discussion

### KEGG enrichment analysis reveals phagosome term enriched in Ag55 cell transcriptome

Growing Ag55 cells are often leaf-shaped with pseudopodia-like structures (Fig. 1A); a shape typical of insect hemocytes that use pseudopodia to contact and surround foreign particles [34]. The transcriptome of Ag55 cells was defined by DNA sequencing cDNA prepared from Ag55 cells. Total paired-end reads obtained per sample from the Illumina HighSeq2000 platform ranged from 16.29 million to 23.11 million, of which 11.76 million to 16.99 million reads had aligned pairs. Mapping Ag55 cell transcripts to an *A. gambiae* reference genome detected transcripts from 10, 320 genes. Transcriptomic studies have arbitrarily divided transcript levels into high, medium and low groups with varying FPKM value range [35–37]. We assigned transcript levels into four groups: high ( $FPKM \geq 200$ ), medium ( $200 < FPKM \geq 10$ ), low ( $10 < FPKM \geq 0.1$ ) and very low ( $0.1 < FPKM > 0$ ) and used high transcript level group for KEGG enrichment analysis using DAVID v6.8. Five KEGG pathway terms: ribosome, oxidative phosphorylation, proteasome, phagosome and glycolysis were enriched (Fig. 1B, Additional file 1).

# Ag55 cells have phagocytic properties and expressed genes of hemocyte-like cells

Enrichment of phagosome KEGG pathway term and hemocyte like morphology led us to analyze whether Ag55 cells have phagocytic properties and hemocyte-like characteristics. Further, Glial cells [38, 39] and ovarian follicle cells [40] have also been shown to work as non-professional phagocytes in Drosophila. Glial cells [38, 39] and ovarian follicle cells mainly mediate apoptotic cell clearance (a process also described as efferocytosis). Baton et al. [41] identified 279 gene transcripts enriched in *A.gambiae* hemocyte relative to adult female mosquitoes. We could assign AGAP identifications to 248 gene transcripts from Baton et al. [41]. Analysis of hemocyte enriched gene transcripts [41] in Ag55 cell transcriptome data detected around 85% (211) of these gene transcripts in Ag55 cells (Fig. 2A, Additional file 2). Further, around 45% (111) of these genes had high to moderate level of transcripts in Ag55 cells (Fig. 2A, Additional file 2).

Smith et al. [42] identified 1128 proteins expressed in *A. gambiae* adult hemocytes so we decided to analyze whether or not the transcripts of these proteins are present in our Ag55 cell transcriptome data. Out of 1128 proteins, 1125 had unique AGAP number. We identified around 95% (1067) of hemocyte expressed protein [42] transcripts in Ag55 cells (Fig. 2B, Additional file 3). Out of 95% identified transcripts, around 71% (795) had high to moderate transcript levels (Fig. 2B, Additional file 3). Presence of hemocyte-expressed transcripts in Ag55 cells led us to analyze the transcript levels of reported hemocyte marker genes [43, 44]. The transcripts of PPO6, SRPN10, LYSC1, PSMD3/Dox-A2, SRPN6, Sp22D and AGAP007314 genes were detected in Ag55 cells (Table 1). LYSC1, PSMD3/Dox-A2 and SRPN10 had high to moderate transcript levels (Table 1).

Table 1: Transcript levels of hemocyte marker genes in Ag55 cells. Hemocyte markers information taken from [41].

Gene Id	Gene name	FPKM Value
AGAP007314	uncharacterized	1.00511
AGAP004977	PPO6	0.0409407
AGAP005246	SRPN10	42.0592
AGAP007347	LYSC1	4722.85
AGAP009082	PSMD3/Dox-A2	96.4581
AGAP009212	SRPN6	7.86527
AGAP005625	Sp22D	107.526

Hemocytes work as professional phagocytes engulfing pathogens, apoptotic cells and dendrite debris

Loading [MathJax]/jax/output/CommonHTML/fonts/TeX/fontdata.js dedicated plasma membrane receptors that

bind to molecules exposed on the surface of pathogens or apoptotic cells. Therefore, we decided to analyze the plasma-membrane phagocytic receptors transcript levels in Ag55 cells (Table 2). High transcript levels ( $\text{FPKM} \geq 200$ ) of SCRC1, nimrodB2 and PGRPLC genes were observed in Ag55 cell transcriptome data (Table 2). SCRC1 belongs to scavenger receptor group of proteins. These are transmembrane proteins and are expressed by both invertebrate and mammalian professional phagocytes [39]. *Anopheles gambiae* SCRC1 homolog in *Drosophila* dSr-Cl binds to bacteria and phagocytose both gram-positive and gram-negative bacteria [45, 46]. In *D. melanogaster* nimrod family genes have been divided into 3 sub-classes nimrodA, B, and C. The nimrodA genes encode for 1 NIM domain, several EGF domains and transmembrane domain. In contrast, nimrodB genes encode for several NIM repeats and no transmembrane domain. Genes in nimrodC subclass encode multiple NIM repeats and a transmembrane domain [47]. The nimrod family genes (draper, and eater orthologs), identified at transcript level in Ag55 cells (Table 2), have been shown to be expressed in hemocytes and are involved in mosquito antibacterial immune response [47].

Table 2: Transcript levels of genes known to encode phagocytic receptor, in Ag55 cells [36].

Gene Id	Gene name	FPKM Value
AGAP011974	SCRC1	360.87
AGAP009762	nimrod B2	340.8256
AGAP005203	PGRPLC	200.699
AGAP006745	Ninjurin	152.875
AGAP000536	PGRPS1	140.15
AGAP005625	SCRASP1/Sp22D	107.526
AGAP005205	PGRPLA	70.8505
AGAP000815	INTB	50.3769
AGAP010133	SCRPQ2	23.9542
AGAP007256	Draper	10.4823
AGAP000307	INT $\alpha$ -PS1	6.15536
AGAP001212	PGRPLB	3.84038
AGAP004847	SCRB7	3.75584
AGAP006343	PGRPS2	2.47051
AGAP009763	nimrod family gene	1.75354
AGAP005552	PGRPLD	1.64555
AGAP004845	SCRB	1.46246
AGAP010233	INT $\beta$ 1	1.40423
AGAP009143	SCRAC1	1.1104
AGAP004118	SCRAL1	0.938871
AGAP002738	SCRB5	0.743612
AGAP003373	SCRB17	0.629896
AGAP000016	SCRB10	0.412842
AGAP006631	SCRASP2	0.316504
AGAP010132	SCRBQ1	0.23563
AGAP004303	INT $\alpha$ -PS	0.126294
AGAP006826	INT $\alpha$ -PS	0.0996884
Loading [MathJax]/jax/output/CommonHTML/fonts/TeX/fontdata.js		0.0962171

Gene Id	Gene name	FPKM Value
AGAP004846	SCRB9	0.071208
AGAP005716	SCRB16	0.0422919
AGAP005725	SCRB3	0.0253694
AGAP001979	SCRASP3	0.0232733
AGAP004643	SCRB6	0.0186534

In *D. melanogaster* draper, nimC1 and eater participate in bacterial binding which in turn leads to phagocytosis by hemocytes [47]. PGRPLC belongs to a family of pattern recognition receptors, which detects peptidoglycans of bacterial cell wall [39]. PGRP-LC is involved in phagocytosis of gram-negative, but not gram-positive bacteria [45]. Silencing of *Anopheles* PGRP-LC reduces *E. coli* engulfment by ~ 60% [45].

Hemocytes are known to express anti-microbial peptides [39] therefore; we decided to analyze presence of anti-microbial peptides in our transcriptome data. We were able to detect the transcripts of defensin (DEF1, 2 and 4), attacin (ATT), cecropin (CEC1 and 3) and gambiaein (GAM1) anti-microbial peptides in our transcriptome data (Table 3). Among the detected anti-microbial peptides transcript CEC1 (FPKM = 89.7283) followed by CEC3 (FPKM = 72.347) had highest transcript levels (Table 3).

Table 3: Transcript levels of genes expressing anti-microbial peptides in Ag55 cells.

Gene Id	Gene name	FPKM Value
AGAP005416	DEF4	0.986614
AGAP005620	ATT	2.63123
AGAP011294	DEF1	0.888614
AGAP004632	DEF2	11.5043
AGAP000693	CEC1	89.7283
AGAP000694	CEC3	72.347
AGAP008645	GAM1	41.5314

## Confocal microscopy and flow-cytometry data confirms uptake of FITC-labeled *E. coli* bioparticles by Ag55 cells

As transcripts (Table 2) of several proteins involved in phagocytosis of Gram-positive and negative Loading [MathJax]/jax/output/CommonHTML/fonts/TeX/fontdata.js ded to confirm whether Ag55 cells phagocytose.

Ag55 cells were tested for the ability to ingest fluorescently tagged E. coli bioparticles. The cultured cells were incubated with FITC-labeled E. coli bioparticles and then the locations of fluorescent particles imaged by confocal microscopy. Figure 3 shows the clustering of E. coli bioparticles in Ag55 cells. Before Ag55 cells were exposed to FITC-E. coli they were treated with lysotracker, an acidophilic dye that localizes to late endosomes and lysosomes [48]. The FITC-labeled E. coli bioparticles internalized and co-localized with Lysotracker deep red in Ag55 cells (Fig. 3C-F). Confocal imaging confirmed the internalization of FITC-E. coli bioparticles. To address the question, what percentage or number of Ag55 cells are internalizing FITC-E. coli bioparticles, we performed flow-cytometry experiments. In control treatments without FITC-E. coli bioparticles, 0.35% Ag55 cells (Fig. 4A) showed uptake of bioparticle but when treated with trypan blue the number decreased to 0.20% (Fig. 4B). The anomaly that controls (Fig. 4A, B) are showing uptake of FITC-E. coli bioparticle may be due to the endogenous fluorescence of Ag55 cells. When exposed to FITC-E. coli, 77.6% of Ag55 cells showed internalization of bacteria bioparticles (Fig. 4C). Further treatment with trypan blue showed reduction in percentage uptake to 73.8% (Fig. 4D). This reduction in uptake may be due to the presence of non-internalized FITC-E. coli bioparticles (Fig. 4C) which was quenched by trypan blue (Fig. 4D) also as FITC quencher. The results from confocal and FACS data suggest that Ag55 cells have phagocytic properties.

## Conclusion

Different cell types have been shown to internalize foreign particles in Drosophila [39]. Hemocyte, a professional phagocyte can be distinguished with non-professional phagocyte (glial, ovarian follicle epithelial and nurse cells) by presence of hemocyte specific markers [44, 45]. We detected the transcripts of hemocyte specific markers in our Ag55 transcriptome data. Further non-professional phagocytes display reduced phagocytic abilities compared to hemocytes [39]. Internalization of FITC-E. coli bioparticles by most of the Ag55 cells (73.8%), presence of anti-microbial peptide and hemocyte-expressed transcripts in Ag55 cell transcriptome data further suggest that Ag55 cells are hemocyte-like.

## Materials And Methods

### Ag55 cell growth and maintenance

Ag55 cell line was originally derived from Anopheles gambiae neonate first instar larvae [29] and gifted by Dr. Paul Linser, University of Florida, USA. Ag55 cells were grown in Leibovitz's L-15 cell culture media (from Sigma) with additional 10% (v/v) fetal bovine serum (FBS, Atlanta Biologicals) and 1% (v/v) penicillin-streptomycin solution (10,000 U/ml and 10 mg/ml, respectively) (Sigma) in 25 cm<sup>2</sup> flasks (Corning) at 28 °C. The cells were grown in the flask until 80% confluence was reached after that the cells were transferred to new flask with fresh media for next (new) generation culture.

### RNA extraction, sequencing and data analysis

RNA extraction, sequencing and data analysis was performed according to Hire et al. [31]. In brief, RNA was extracted from Ag55 cells using TRIzol (Ambion). Approximately,  $1 \times 10^7$  confluent cells (1 flask of 25 cm<sup>2</sup>) were homogenized in TRIzol reagent (200 µl) and further processed for RNA extraction following the manufacturer's instructions (Ambion). Extraction of RNA from Ag55 cells was replicated three times. The purity and concentrations of RNA samples were determined using a NanoDrop spectrophotometer (N-1000) before dispatching samples for quality control and sequencing to the Georgia Genome Facility (GGF), University of Georgia.

At the GGF, pre-sequencing steps such as RNA integrity determination, Poly (A) enrichment of mRNA followed by cDNA synthesis and library preparation were performed. Sequencing was carried out using 100 bp paired-end Illumina HiSeq 2000 v3 platform.

For RNA-seq analysis, Trapnell et al. [48] protocol was followed. Based on the FastQC result, the pre-processing step of trimming the 3' and 5' end sequences was omitted. *A. gambiae* genome (Anopheles-gambiae-PEST\_CHROMOSOMES\_AgamP4.fa.gz) was downloaded from (VectorBase) and used as a reference for mapping the transcripts. Each dataset was independently mapped to the reference using Tophat v2.0.13 [49, 50], which uses Bowtie2 [51] as an aligner. Post alignment, Cufflinks v2.2.1 [52] was used to estimate the expression values of the transcripts in FPKM (Fragments Per Kilobase per Million mapped reads) with the Cuffdiff 2 default geometric normalization. The expression levels (in FPKM) of genes of interest were extracted from genes.fpkm\_tracking and isoforms.fpkm\_tracking.

## KEGG process term enrichment analysis

KEGG enrichment analysis was performed using DAVID v6.8 algorithm [53, 54]. Only gene transcripts which FPKM  $\geq 200$  in Ag55 cells were selected for enrichment analysis. Only those KEGG pathway terms were selected whose fold enrichment was  $> 2$  and p-value  $< 0.05$ .

## Confocal imaging for determining the morphology of live Ag55 cells

Ag55 cells ( $1 \times 10^6$ ) were seeded in chambered coverslips (ibidi, GmbH) and after three hours the Ag55 cells were incubated with Hoechst stain (ThermoFisher) and Nile red for 10 min as background stains. After 10 min incubation, live Ag55 cells were observed with a LSM 710 confocal microscope (Carl Zeiss).

## Ag55 cell phagocytosis assay

Ag55 cells ( $0.5 \times 10^6$ ) were seeded in 4 chambered glass slides. After adhesion of the cells to the chambered glass slide, the cells were incubated with 10 nM Lysotracker for 2 hr at 28°C. The cells were then washed three times with cell media and incubated with FITC-labeled *E. coli* bioparticles (ThermoFisher scientific) at a ratio of 1:50 (cell/FITC-labeled *E. coli* bioparticles) for 35 min. After incubation, cells were washed three times with 1 × PBS (phosphate buffer saline (137 mM NaCl, 2.7 mM KCl, 4.3 mM Na<sub>2</sub>HPO<sub>4</sub>, and 1.47 mM KH<sub>2</sub>PO<sub>4</sub>). Subsequently, the cells were fixed with 4%

Loading [MathJax]/jax/output/CommonHTML/fonts/TeX/fontdata.js ] n. After fixation cells were washed times with 1

× PBS and incubated with 8.1 µM Hoechst stain (nuclear stain) for 10 min in dark. The cells were then washed 3 times with 1 × PBS and observed under an LSM 710 confocal microscope (Carl Zeiss).

## Flow cytometry assay

Flow cytometry assay was performed according to Hua et al. [55]. In brief, Ag55 cells ( $1 \times 10^6$ /well) were seeded in 6-well plate and incubated with 10-fold of FITC bacteria. After incubated for 2 hours at 28 °C, the culture medium was discarded. The cells were washed with culture medium three times to remove the free FITC-bacteria and trypan blue (0.2%) was used to quenching FITC outside of the cells at room temperature for 10 min [46, 56]. Finally, the cells were washed with culture medium three time and suspended in 1 ml of medium for FACS analyses using a FACSCalibur (BD Life Sciences

## Availability of RNA sequencing data

The data discussed in the manuscript have been submitted to NCBI's Gene Expression Omnibus (GEO) and are accessible through GEO series accession number GSE85643 (<http://www.ncbi.nlm.nih.gov/geo/query/acc.cgi?acc=GSE85643>). BioProject Id: PRJNA338993 and SRA Id: SRP082173.

## Abbreviations

**KEGG:** Kyoto Encyclopedia of Genes and Genomes; **RNAi:** RNA interference; **FPKM:** Fragments per kilo base per million mapped reads; **SRPN:** Serpin; **PPO6:** Prophenoloxidase 6; **LYSC1:** Lysozyme C1; **SCRC1:** Scavenger receptor class C; **PGRPLC:** Peptidoglycan recognition protein LC; **FACS:** Fluorescence-activated cell sorting; **FITC:** Fluorescein isothiocyanate

## Declarations

### Competing Interests

The authors declare no competing interests exist

### Author's contributions

R.M., M.J.A. and D.C. designed research; R.M. and U.B. performed bioinformatic analyses; R.M. and G.H. performed confocal microscopy; G.H. performed flow-cytometry experiment; R.M. and M.J.A. wrote the paper; M.J.A, D.C., G.H. and U.B. reviewed and helped improving the manuscript. All authors read and approved the manuscript.

### Acknowledgments

We thank Drs. Judith Willis, Maria-Helena Silva Filha, and Antonio Mauro-Rezende. The project was supported by Hatch Project \_\_\_\_ to Dr. Michael Adang.

## References

1. Organization WH: World malaria report 2018. In: WHO: Geneva. 2018.
2. Dimopoulos G, Richman A, Muller HM, Kafatos FC. Molecular immune responses of the mosquito *Anopheles gambiae* to bacteria and malaria parasites. Proc Natl Acad Sci USA. 1997;94(21):11508-11513.
3. Waldock J, Olson K, Christophides G. Anopheles gambiae antiviral immune response to systemic O'nyong-nyong infection. PLoS Negl Trop Dis. 2012;6(3):e1565.
4. Walker T, Jeffries CL, Mansfield KL, Johnson N. Mosquito cell lines: history, isolation, availability and application to assess the threat of arboviral transmission in the United Kingdom. Parasites & vectors. 2014;7:382.
5. Parish LA, Garver LS, Colquhoun DR, Mohien CU, Weissbrod E, Dinglasan RR. Dissecting mosquito-parasite interactions through molecular biology and biochemistry: genomic, proteomic and glycomic analyses. Poole, UK: Caister Academic Press; 2013.
6. Sim S, Dimopoulos G. Dengue virus inhibits immune responses in *Aedes aegypti* cells. PloS one. 2010;5(5):e10678.
7. Juárez-Martínez AB, Vega-Almeida TO, Salas-Benito M, García-Espitia M, De Nova-Ocampo M, Del Ángel RM, Salas-Benito JS. Detection and sequencing of defective viral genomes in C6/36 cells persistently infected with dengue virus 2. Arch Virol. 2013;158(3):583-599.
8. Wilkins S, Billingsley PF. Mosquito cell line glycoproteins: an unsuitable model system for the *Plasmodium* ookinete-mosquito midgut interaction? Parasites & vectors. 2010;3(1):22.
9. Schnettler E, Donald C, Human S, Watson M, Siu RW, McFarlane M, Fazakerley J, Kohl A, Frakoudis R. Knockdown of piRNA pathway proteins results in enhanced Semliki Forest virus production in mosquito cells. J Gen Virol. 2013;94(Pt 7):1680-1689.
10. Kuno G. Host range specificity of flaviviruses: correlation with in vitro replication. J Med Entomol. 2007;44(1):93-101.
11. Lawrie C, Uzcategui N, Armesto M, Bell-Sakyi L, Gould E. Susceptibility of mosquito and tick cell lines to infection with various flaviviruses. Med Vet Entomol. 2004;18(3):268-274.
12. Hobson-Peters J, Yam A, Lu J, Setoh YX, May FJ, Kurucz N, Walsh S, Prow NA, Davis SS, Weir R. A new insect-specific flavivirus from northern Australia suppresses replication of West Nile virus and Murray Valley encephalitis virus in co-infected mosquito cells. PloS one. 2013;8(2):e56534.
13. Haddow A, Guzman H, Popov V, Wood T, Widen S, Haddow A, Tesh R, Weaver S. First isolation of *Aedes* flavivirus in the Western Hemisphere and evidence of vertical transmission in the mosquito *Aedes (Stegomyia) albopictus* (Diptera: Culicidae). Virology. 2013;440(2):134-139.
14. Al-Olayan E, Beetsma A, Butcher G, Sinden R, Hurd H. Complete development of mosquito phases of the malaria parasite *in vitro*. Science. 2002;295(5555):677-679.
15. Sidén-Kiamos I, Vlachou D, Margos G, Beetsma A, Waters A, Sinden R, Louis C. Distinct roles for loading [MathJax]/jax/output/CommonHTML/fonts/TeX/fontdata.js information of *Plasmodium berghei*. J Cell Sci.

2000;113(19):3419-3426.

16. O'Neal M, Posner B, Coates C, Abrams J. A cell-based screening platform identifies novel mosquitocidal toxins. *J Biomolec Screen*. 2013;18(6):688-694.
17. Cherry S. Genomic RNAi screening in *Drosophila* S2 cells: what have we learned about host-pathogen interactions? *Curr Opin Microbiol*. 2008;11(3):262-270.
18. Echeverri C, Perrimon N. High-throughput RNAi screening in cultured cells: a user's guide. *Nat Rev Genet*. 2006;7(5):373-384.
19. Boutros M, Kiger A, Armknecht S, Kerr K, Hild M, Koch B, Haas S, Paro R, Perrimon N, Consortium H. Genome-wide RNAi analysis of growth and viability in *Drosophila* cells. *Science*. 2004;303(5659):832-835.
20. Cherbas L, Gong L. Cell lines. *Methods*. 2014;68(1):74-81.
21. Hu X, Cherbas L, Cherbas P. Transcription activation by the ecdysone receptor (EcR/USP): Identification of activation functions. *Molec Endocrin*. 2003;17(4):716-731.
22. Cherbas L, Hu X, Zhimulev I, Belyaeva E, Cherbas P. EcR isoforms in *Drosophila*: testing tissue-specific requirements by targeted blockade and rescue. *Development*. 2003;130(2):271-284.
23. Fehon R, Kooh P, Rebay I, Regan C, Xu T, Muskavitch M, Artavanistsakonas S. Molecular-interactions between the protein products of the neurogenic loci notch, delta, 2 EGF-homologous genes in *Drosophila*. *Cell*. 1990;61(3):523-534.
24. Lombardo F, Ghani Y, Kafatos F, Christophides G. Comprehensive genetic dissection of the hemocyte immune response in the malaria mosquito *Anopheles gambiae*. *Plos Pathogens*. 2013;9(1).
25. Muller H, Dimopoulos G, Blass C, Kafatos F. A hemocyte-like cell line established from the malaria vector *Anopheles gambiae* expresses six prophenoloxidase genes. *J Biol Chem*. 1999;274(17):11727-11735.
26. Meister S, Kanzok S, Zheng X, Luna C, Li T, Hoa N, Clayton J, White K, Kafatos F, Christophides G et al. Immune signaling pathways regulating bacterial and malaria parasite infection of the mosquito *Anopheles gambiae*. *Proc Natl Acad Sci USA*. 2005;102(32):11420-11425.
27. Dimopoulos G, Christophides G, Meister S, Schultz J, White K, Barillas-Mury C, Kafatos F. Genome expression analysis of *Anopheles gambiae*: responses to injury, bacterial challenge, and malaria infection. *Proc Natl Acad Sci USA*. 2002;99(13):8814-8819.
28. Levashina E, Moita L, Blandin S, Vriend G, Lagueux M, Kafatos F. Conserved role of a complement-like protein in phagocytosis revealed by dsRNA knockout in cultured cells of the mosquito, *Anopheles gambiae*. *Cell*. 2001;104(5):709-718.
29. Pudney M, Varma M, Leake C. Establishment of cell lines from larvae of culicine (*Aedes* species) and Anopheline mosquitoes. *TCA Manual*. 1979;5:997-1002.
30. Rasgon J, Ren X, Petridis M. Can *Anopheles gambiae* be infected with Wolbachia pipiensis? Insights from an *in vitro* system. *Appl Environ Microbiol*. 2006;72(12):7718-7722.

31. Hire R, Hua G, Zhang Q, Mishra R, Adang M. *Anopheles gambiae* Ag55 cell line as a model for *Lysinibacillus sphaericus* Bin toxin action. *J Invertbr Pathol.* 2015;132:105-110.
32. Konet D, Anderson J, Piper J, Akkina R, Suchman E, Carlson J. Short-hairpin RNA expressed from polymerase III promoters mediates RNA interference in mosquito cells. *Insect Molec Biol.* 2007;16(2):199-206.
33. Smith K, Linser P. Silencing of carbonic anhydrase in an *Anopheles gambiae* larval cell line, Ag55. *RNAi Gene Silencing.* 2009;5(1):345-350.
34. Kwon H, Bang K, Cho S. Characterization of the hemocytes in Larvae of *Protaetia brevitarsis seuensis*: involvement of granulocyte-mediated phagocytosis. *PloS one.* 2014;9(8):e103620.
35. Ghaffari P, Mardinoglu A, Asplund A, Shoaei S, Kampf C, Uhlen M, Nielsen J. Identifying anti-growth factors for human cancer cell lines through genome-scale metabolic modeling. *Scientific reports.* 2015;5(1):1-10.
36. Flegel C, Schöbel N, Altmüller J, Becker C, Tannapfel A, Hatt H, Gisselmann G. RNA-Seq analysis of human trigeminal and dorsal root ganglia with a focus on chemoreceptors. *PloS one.* 2015;10(6).
37. Indoliya Y, Tiwari P, Chauhan AS, Goel R, Shri M, Bag SK, Chakrabarty D. Decoding regulatory landscape of somatic embryogenesis reveals differential regulatory networks between japonica and indica rice subspecies. *Scientific reports.* 2016;6:23050.
38. Shklover J, Levy-Adam F, Kurant E: Apoptotic cell clearance in development. In: *Curr Top Dev Biol.* vol. 114: Elsevier; 2015: 297-334.
39. Melcarne C, Lemaitre B, Kurant E. Phagocytosis in *Drosophila*: from molecules and cellular machinery to physiology. *Insect Biochem Molec Biol.* 2019;109:1-12.
40. Serizier S, McCall K. Scrambled eggs: Apoptotic cell clearance by non-professional phagocytes in the *Drosophila* ovary. *Front Immunol.* 2017;8:1642.
41. Baton L, Robertson A, Warr E, Strand M, Dimopoulos G. Genome-wide transcriptomic profiling of *Anopheles gambiae* hemocytes reveals pathogen-specific signatures upon bacterial challenge and *Plasmodium berghei* infection. *BMC Genom.* 2009;10(1):257.
42. Smith R, King J, Tao D, Zelezniak O, Brando C, Thallinger G, Dinglasan R. Molecular profiling of phagocytic immune cells in *Anopheles gambiae* reveals integral roles for hemocytes in mosquito innate immunity. *Molec Cell Prot.* 2016;15(11):3373-3387.
43. Castillo J, Robertson A, Strand M. Characterization of hemocytes from the mosquitoes *Anopheles gambiae* and *Aedes aegypti*. *Insect Biochem Molec Biol.* 2006;36(12):891-903.
44. Severo M, Landry J, Lindquist R, Goosmann C, Brinkmann V, Collier P, Hauser A, Benes V, Henriksson J, Teichmann S. Unbiased classification of mosquito blood cells by single-cell genomics and high-content imaging. *Proc Natl Acad Sci USA.* 2018;115(32):E7568-E7577.
45. Pearson A, Lux A, Krieger M. Expression cloning of dSR-CI, a class C macrophage-specific scavenger receptor from *Drosophila melanogaster*. *Proc Nat Acad Sci USA.* 1995;92(9):4056-4060.

46. Rämet M, Manfruelli P, Pearson A, Mathey-Prevot B, Ezekowitz R. Functional genomic analysis of phagocytosis and identification of a *Drosophila* receptor for *E. coli*. *Nature*. 2002;416(6881):644-648.
47. Estévez-Lao T, Hillyer J. Involvement of the *Anopheles gambiae* Nimrod gene family in mosquito immune responses. *Insect Biochem Molec Biol*. 2014;44:12-22.
48. Trapnell C, Roberts A, Goff L, Pertea G, Kim D, Kelley D, Pimentel H, Salzberg S, Rinn J, Pachter L. Differential gene and transcript expression analysis of RNA-seq experiments with TopHat and Cufflinks. *Nat Protoc*. 2012;7(3):562-578.
49. Trapnell C, Pachter L, Salzberg S. TopHat: discovering splice junctions with RNA-Seq. *Bioinformatics*. 2009;25(9):1105-1111.
50. Kim D, Pertea G, Trapnell C, Pimentel H, Kelley R, Salzberg S. TopHat2: accurate alignment of transcriptomes in the presence of insertions, deletions and gene fusions. *Genome Biol*. 2013;14(4).
51. Langmead B, Trapnell C, Pop M, Salzberg S. Ultrafast and memory-efficient alignment of short DNA sequences to the human genome. *Genome Biol*. 2009;10(3).
52. Trapnell C, Williams B, Pertea G, Mortazavi A, Kwan G, van Baren M, Salzberg S, Wold B, Pachter L. Transcript assembly and quantification by RNA-Seq reveals unannotated transcripts and isoform switching during cell differentiation. *Nat Biotechnol*. 2010;28(5):511-U174.
53. Sherman B, Lempicki R. Systematic and integrative analysis of large gene lists using DAVID bioinformatics resources. *Nat Protocol*. 2009;4(1):44-57.
54. Huang D, Sherman B, Lempicki R. Bioinformatics enrichment tools: paths toward the comprehensive functional analysis of large gene lists. *Nucleic Acids Res*. 2008;37(1):1-13.
55. Hua G, Jurat-Fuentes J, Adang M. Fluorescent-based assays establish *Manduca sexta* Bt-R<sub>1a</sub> cadherin as a receptor for multiple *Bacillus thuringiensis* Cry1A toxins in *Drosophila* S2 cells. *Insect Biochem Molec Biol*. 2004;34(3):193-202.
56. Kocks C, Cho JH, Nehme N, Ulvila J, Pearson AM, Meister M, Strom C, Conto SL, Hetru C, Stuart LM. Eater, a transmembrane protein mediating phagocytosis of bacterial pathogens in *Drosophila*. *Cell*. 2005;123(2):335-346.

## Figures

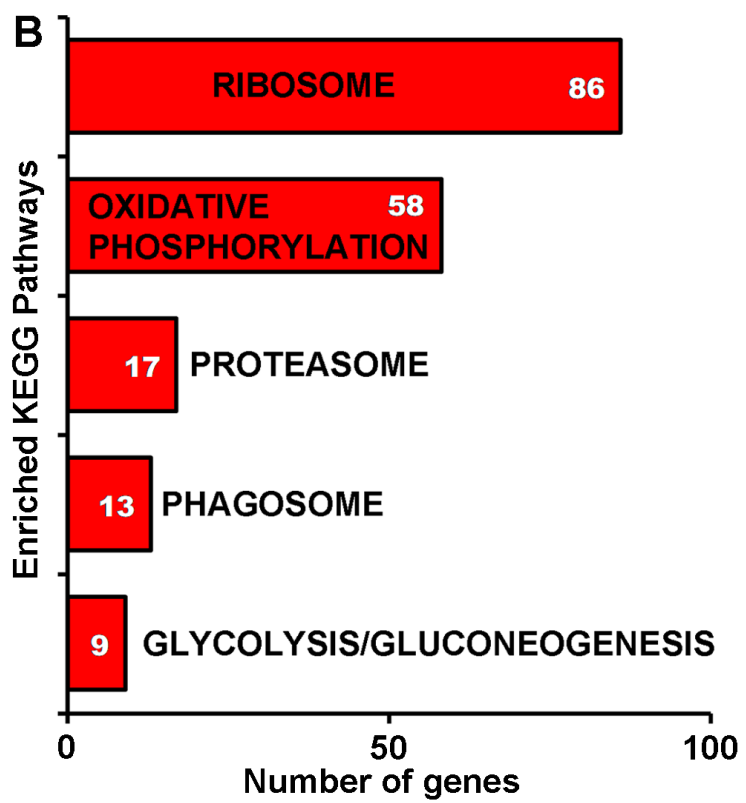
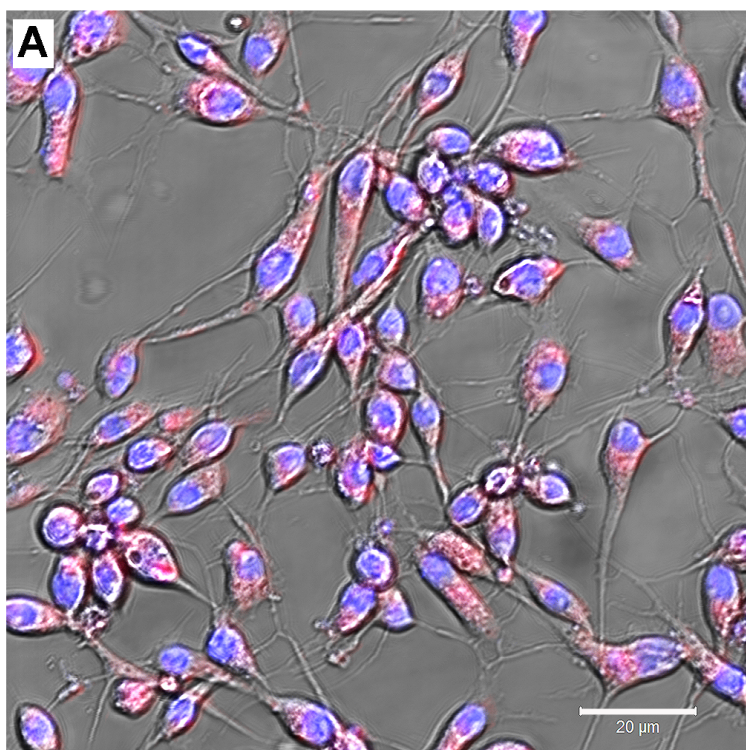


**Figure 1**

Appearance of live Ag55 cells (A), and enriched KEGG pathways in Ag55 cell transcriptome (B). Panel A shows the leaf-shaped appearance of some Ag55. Ag55 cells were seeded in a chambered coverslip and stained with Hoechst stain to visualize nuclei and Nile red to stain lipids. Cells were observed under LSM 710 confocal microscope (Carl Zeiss) at 20 X magnification. Panel B shows Enriched KEGG pathways of

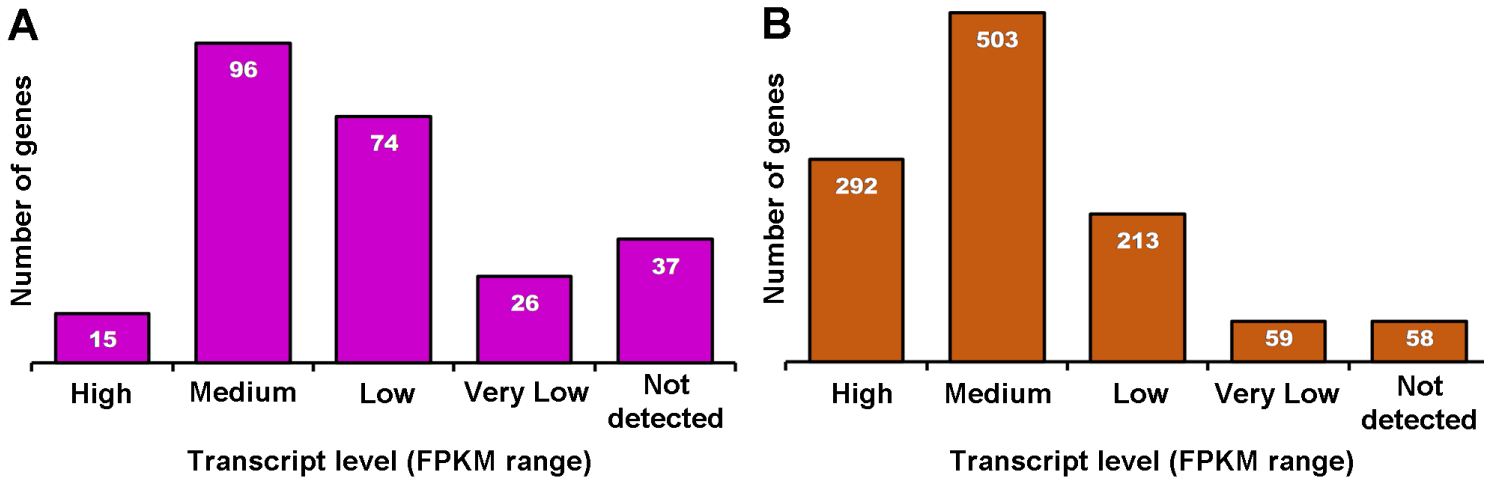


**Figure 2**

Transcript levels of female *A. gambiae* hemocyte-enriched genes (A) [38] and hemocyte proteome (B) [39] in Ag55 cells. Panel A shows the number of genes in Ag55 cells identified by Baton et al. [38] as being enriched in hemocytes. Panel B shows the number of gene transcripts reported in Smith et al. [39] in their analysis of the hemocyte proteome. Arbitrarily assigned transcript level groups are high ( $\text{FPKM} \geq 200$ ), medium ( $200 < \text{FPKM} \geq 10$ ), low ( $10 < \text{FPKM} \geq 0.1$ ) and very low ( $0.1 < \text{FPKM} > 0$ ).

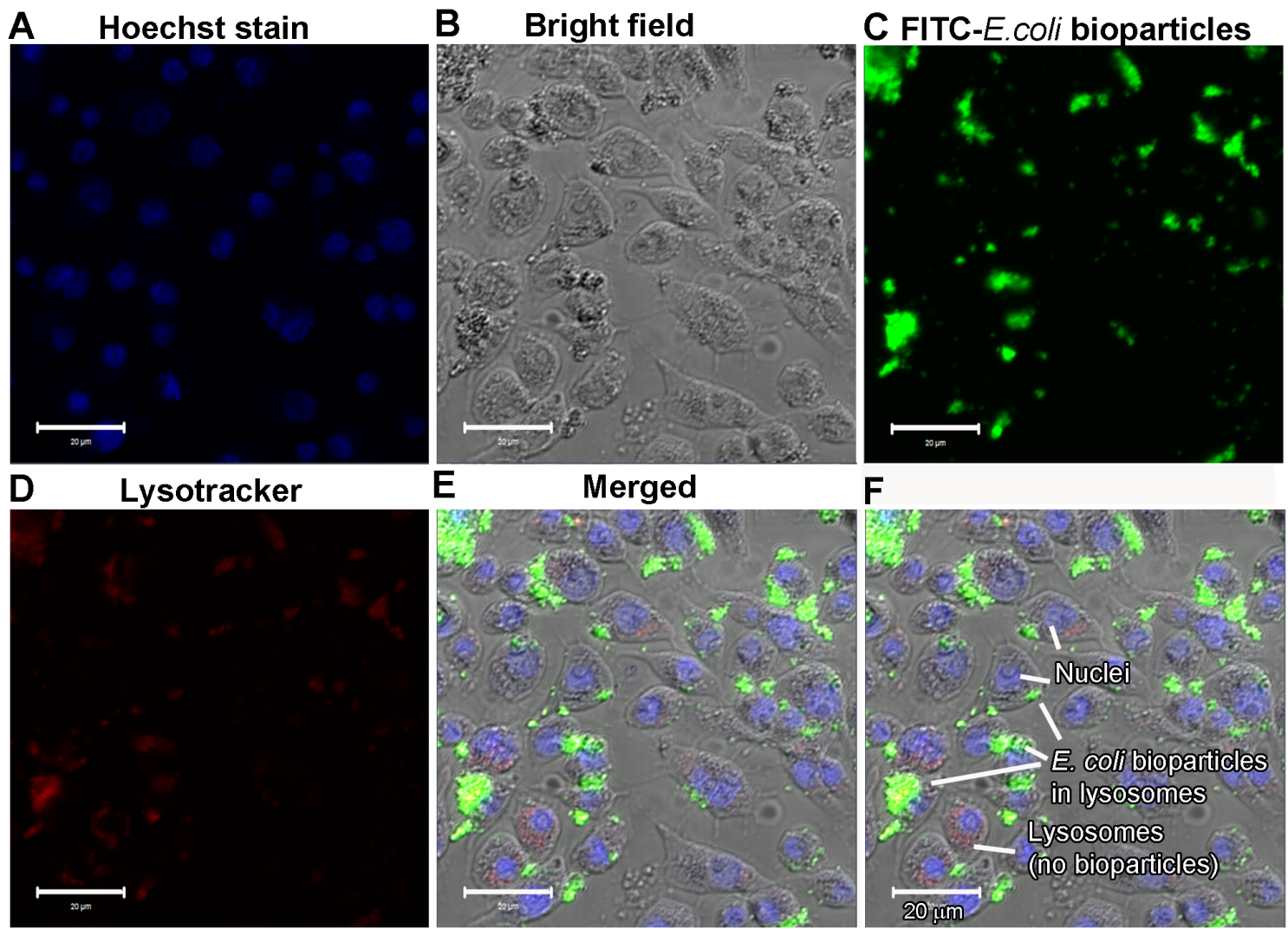


**Figure 3**

Ag55 cells phagocytose *E. coli* bioparticles. Adherent Ag55 cells in 4 chambered glass slides were incubated with 10 nM Lysotracker for 2 hr at 28°C. After washing the cells were incubated with FITC-labeled *E. coli* bioparticles for 35 min. Cells were washed with and fixed with 4% paraformaldehyde for 20 min, washed again and incubated with 8.1 μM Hoechst stain for 10 min in dark. The cells were further washed with 1× PBS and observed under an LSM 710 confocal microscope (Carl Zeiss). Images were taken at 20X-magnification. A: Hoechst stain: used to stain the nuclei (Blue), B: Bright field, C: FITC-labeled *E. coli* bioparticles (Green fluorescence), D: Lysotracker deep red: an acidophilic dye that localizes to late endosomes and lysosomes. E and F: Merged image: shows co-localization of lysotracker deep red and FITC-labeled *E. coli* in late endosome or lysosome suggesting internalization of FITC- *E. coli* bioparticle by Ag55 cells.

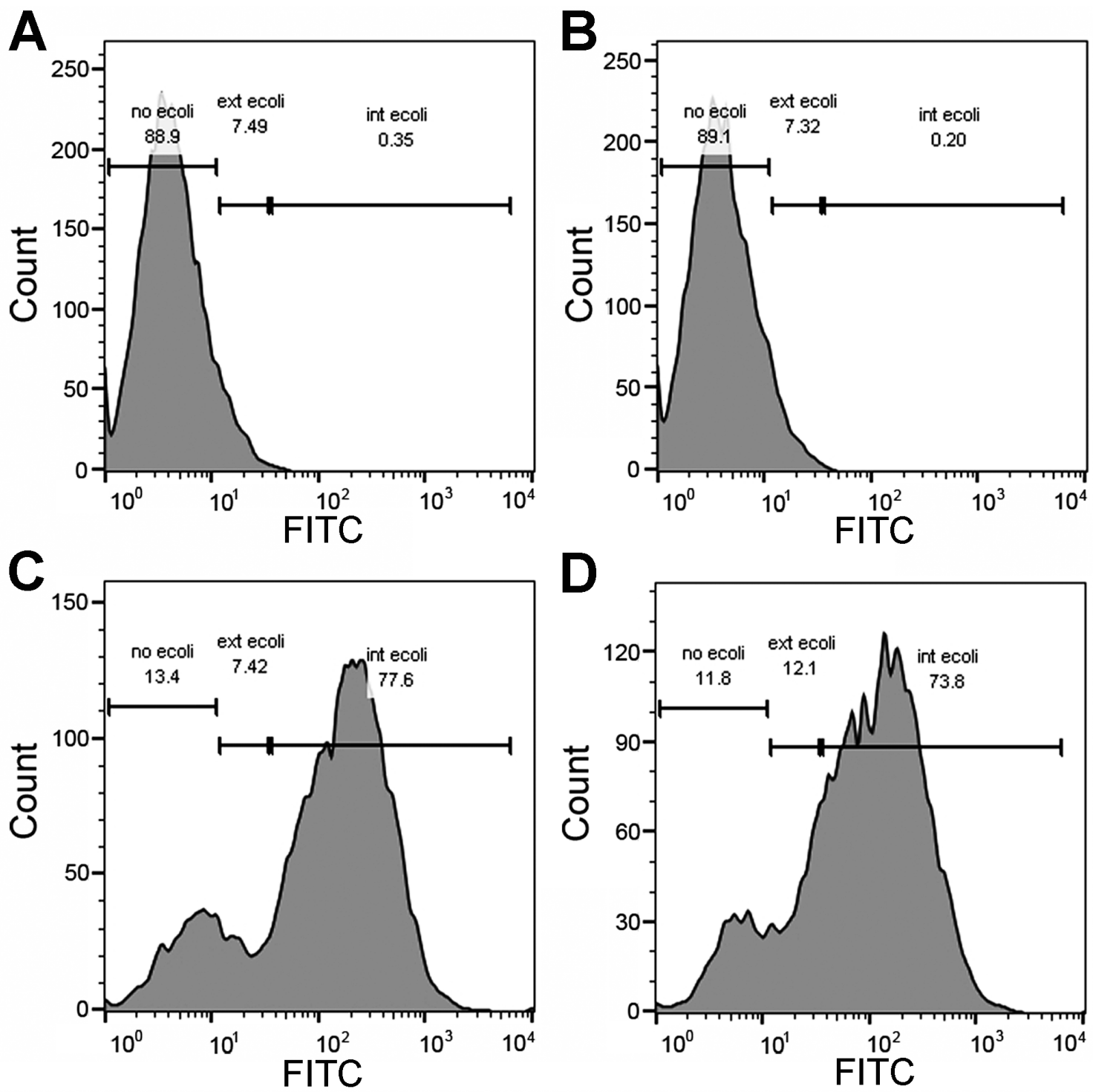


**Figure 4**

Quantification of phagocytosis of FITC-E.coli bioparticles by FACS. Panels A shows the background autofluorescence of Ag55 cells with no FITC-E.coli. As shown in Panel B, the addition of Trypan blue (a FITC fluorescence quenching agent) had no effect on Ag55 cell autofluorescence. Panel C shows the FACS scan of Ag55 cells with internalized FITC-E.coli after Trypan blue quenching of external FITC-E. coli.

## Supplementary Files

Loading [MathJax]/jax/output/CommonHTML/fonts/TeX/fontdata.js

This is a list of supplementary files associated with this preprint. Click to download.

- [Additionalfile2.xlsx](#)
- [Additionalfile3.xlsx](#)
- [Additionalfile1.xlsx](#)